

## Dynamic steady-state tertiary creep in a Nickel-base single crystal superalloy at high temperatures

NIRMAL K. SINHA

*Institute for Aerospace Research, National Research Council Canada, Building M-13, 1200 Montreal Road, Ottawa, Ontario, Canada K1A 0R6*

*E-mail: nirmal.sinha@nrc-cnrc.gc.ca*

**Published online:** 1 November 2005

Nickel-base single crystal (SX) blades, oriented along the [0 0 1] crystallographic direction, were introduced for gas turbine engines in 1980 [1, 2]. Creep resistance of SX materials is derived from the large volume fraction, about 70%, of ordered cubical  $\gamma'$  precipitates in a disordered  $\gamma$  matrix. Since the  $\gamma/\gamma'$  morphology changes during creep, considerable attention has been paid to this topic [1, 3]. Because SX materials exhibit high stress sensitivity and large elongation, the increase in stress, due to the reduction in the cross-sectional area during creep, must control the strain rate and the time to rupture for constant load tests. The objective of this letter is to present our study on this subject. Both experimental and analytical techniques presented here are applicable in general to other materials exhibiting high ductility.

The “third generation” CMSX-10 with a nominal composition (wt.%) of 2Cr, 3Co, 0.4Mo, 6Re, 5W, 5.7Al, 0.2Ti, 8Ta, 0.1Nb, 0.03Hf, balance Ni [2] was used. Creep specimens, with a nominal diameter of 4.0 mm and a uniform gauge section of 25 mm, were prepared from fully heat-treated [0 0 1]-oriented bars. The  $\gamma'$  precipitates had average edge dimensions of about 0.5  $\mu\text{m}$  and there were rows of spherical pores, up to 25  $\mu\text{m}$  in diameter, aligned parallel to the growth direction.

Six constant load tests, for an initial stress  $\sigma_i$  of 700 MPa, were performed in air at 1073 to 1273 K (800–1000°C)  $\pm$  1 K using a single lever dead-load system, a three-zone furnace and an extensometer. Out of these six tests, two rupture tests were performed first at 1123 K and 1173 K to determine the fracture times and strains (19% and 18% at 1123 K and 1173 K respectively). Four strain relaxation (creep) and recovery tests (SRRT) [4] for relaxation times,  $t_{\text{rlx}}$  required to reach a total strain of 15% (close to fracture), were then performed at 1073 K, 1148 K, 1223 K and 1273 K. SRRT involves the application of the load as rapidly as possible, deforming a specimen for  $t_{\text{rlx}}$ , and then removing the load fully and rapidly, but keep monitoring the strain for a long time until no further strain recovery is noticed. SRRTs allow determination of elastic, delayed elastic and viscous components of strain as functions of  $t_{\text{rlx}}$ . Only the strain relax-

ation results of these tests will be presented and discussed here.

Fig. 1 shows all the strain relaxation curves. The average value of the bulk Young's modulus,  $E = 110$  GPa, obtained from the initial elastic strain,  $\varepsilon_e$ , agreed with the expected range for the [0 0 1]-orientation at these temperatures [3, 5]. This allowed the estimation of creep strain,  $\varepsilon_c (= \varepsilon - \varepsilon_e)$ , where  $\varepsilon$  is the total strain. The high stress of 700 MPa, equivalent to  $6.4 \times 10^{-3} E$ , was chosen to avoid complexities of  $\gamma'$  rafting [6, 7]. The fracture strains for the two tests bear strong similarities with those of the “second generation” alloy CMSX-4 for lower stresses, 130 to 400 MPa, at 1273 K [7].

Assuming incompressibility during creep, the actual stress,  $\sigma_A$  was estimated from  $\sigma_A = \sigma_i (1 + \varepsilon_c)$ . This gives, for example, the fracture stress,  $\sigma_{Af}$  of 833 MPa for the test at 1123 K. It would be appropriate to mention here that the specimen cross-sectional shape after the tests was found to be slightly elliptical. For example, the major- and the minor-axis of the specimen tested at 1148 K was 3.76 mm and 3.70 mm respectively near the middle of the specimen – giving a small but measurable eccentricity of 0.183. This does not necessarily mean asymmetry in the load axis and, in fact, is expected due to a number of active slip systems in cubic materials, as reported for SX alloy SRR99 in [8].

Fig. 2 shows the strain rate-time,  $\dot{\varepsilon} - t$  and  $\sigma_A - t$  curves for the test at 1223 K (950 °C). It shows that  $\dot{\varepsilon}$  changes with time in a complex manner similar to observations in CMSX-4 [9, 10]. However, the monotonically increasing  $\sigma_A$  suggests that the conventional approach of plotting  $\dot{\varepsilon} - \varepsilon_c$  curves for analytical purposes (assuming constant stress) violates the basic principles of experimental physics.

The relationship between  $\dot{\varepsilon}$  and  $\sigma_A$  for the results in Fig. 2 and plotted in Fig. 3 clearly shows that the ‘tertiary’ or the ‘time-wise accelerating’ stage represents a “stress-wise dynamic steady state” (broken line in Fig. 3). Note the high regression coefficient,  $R^2$  of 0.997. Similar observations were also made at other temperatures (Fig. 4). The test at 1173 K shows some inconsistency due to some

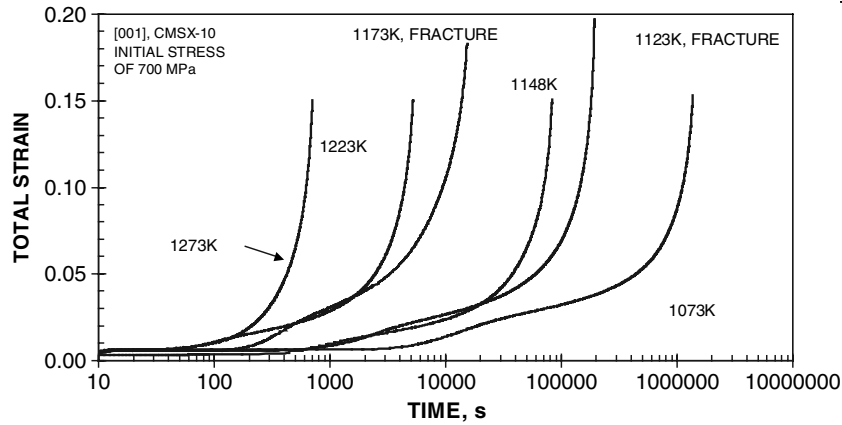


Figure 1 Experimental strain relaxation curves for [001]-oriented CMSX-10 for constant load tests at initial stress of 700 MPa; tests at 1173 and 1123 K deformed to fracture.

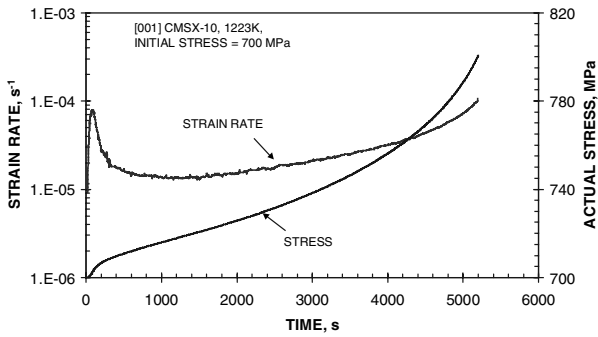


Figure 2 Strain rate (left y-axis) and actual stress (right y-axis) for the test at an initial stress of 700 MPa and 1223 K.

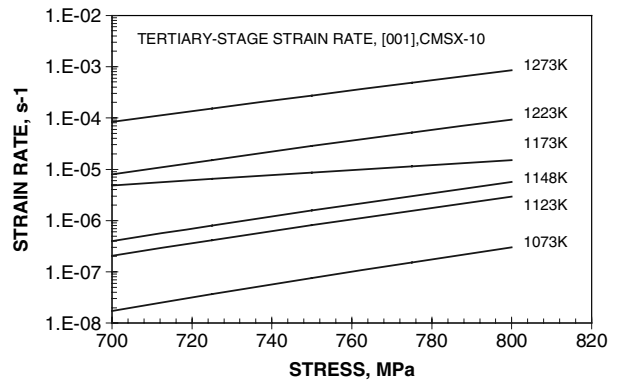


Figure 4 'Tertiary-stage' stress (actual) dependence of strain rate for [001]-oriented CMSX-10 obtained from constant load tests with initial stress of 700 MPa.

data logging problems, but it is included here to show that nothing is perfect in experimental life. Fig. 4 shows that one creep rupture test or a long-term SRRT provides the  $\sigma_A - \dot{\epsilon}$  relationship over a range of stresses (100 MPa in the present series) and suggests an economic, time saving experimental scheme for expensive SX materials.

The results in Fig. 4 were used to make a master curve in the form of a normalized power-law with a shift function,  $S_{1,2}$ , originally developed for directionally solidified (DS)

transversely isotropic polycrystalline ice at temperatures  $> 0.9T_m$  where  $T_m$  is the melting point in Kelvin [11]:

$$\dot{\epsilon} = \dot{\epsilon}_{A(1)}(\sigma_A/\sigma_1)^{h(A)}S_{1,2} \quad (1a)$$

$$S_{1,2} = \exp\{(Q/R)(1/T_2 - 1/T_1)\} \quad (1b)$$

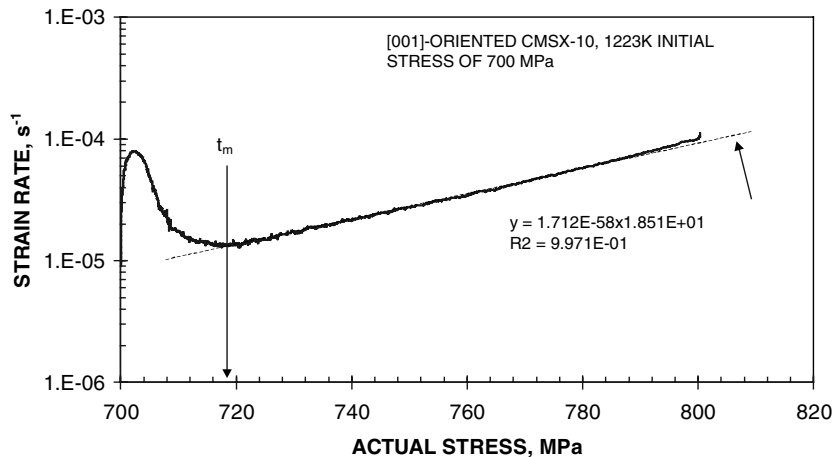


Figure 3 Dependence of strain rate on actual stress for the results in Fig. 2.

where  $\sigma_1$  is the unit stress (=1 MPa) and  $n(A)$  is the stress exponents. ‘A’ implies actual stress and  $T_1, T_2$  are temperatures in Kelvin. The coefficient  $\dot{\epsilon}_{A(1)}$  is interpreted as the equivalent creep rate for unit stress at  $T_1$ .  $Q$  is the apparent creep activation energy (in J mole<sup>-1</sup>) and  $R$  is the universal gas constant (= 8.32 J mole<sup>-1</sup>K<sup>-1</sup>).

If  $\dot{\epsilon}(T_{\text{ref}})$  and  $\dot{\epsilon}(T)$  are the strain rates, for a given stress  $\sigma_A$ , at a reference temperature  $T_{\text{ref}}$  and another temperature  $T$  respectively, then Equation 1a and b give  $S_{\text{ref},T}$  for  $\sigma_A$  as:

$$S_{\text{ref},T} = \dot{\epsilon}(T_{\text{ref}})/\dot{\epsilon}(T) = \exp\{Q/R(1/T - 1/T_{\text{ref}})\} \quad (2)$$

Equation 2 was used to determine  $Q$ . It was found to be independent of stress in the 700–800 MPa range. No systematic variations in  $Q$  were noticed between 1073 K and 1223 K; the average value was 430 kJ mole<sup>-1</sup>. This

is comparable to 495 kJ mole<sup>-1</sup> reported for a “first generation” alloy, CMSX-3 [12] and 435 kJ mole<sup>-1</sup> for a “second generation” alloy, CMSX-4 [10]. However, we noticed a sharp increase to 590 kJ mole<sup>-1</sup> between 1223 K and 1273 K. A change in  $n(A)$ , from 17.4 at 1273 K to 21.4 at 1073 K, was noticed, but  $\dot{\epsilon}_{A(1)}$  also varied. They may reflect the scatter in the material and/or data. High  $n(A)$  value for minimum creep rate ( $\dot{\epsilon}_{\text{min}}$ ) of 13, 17 and 16 respectively for [0 0 1]-, [011]- and [111]-orientation has been reported for CMSX-10 at 1123 K [13]. It is not certain at this stage whether high  $n(A)$  values reflect creep damage enhancement arising from the growth and elongation of the pores and the cracks associated with these pores (Fig. 5). Microstructural observations were and are being made using optical and scanning electron microscope.

Since the primary stages of creep (increasing and decreasing rates in Fig. 2) are complex [3, 9, 10] and involve

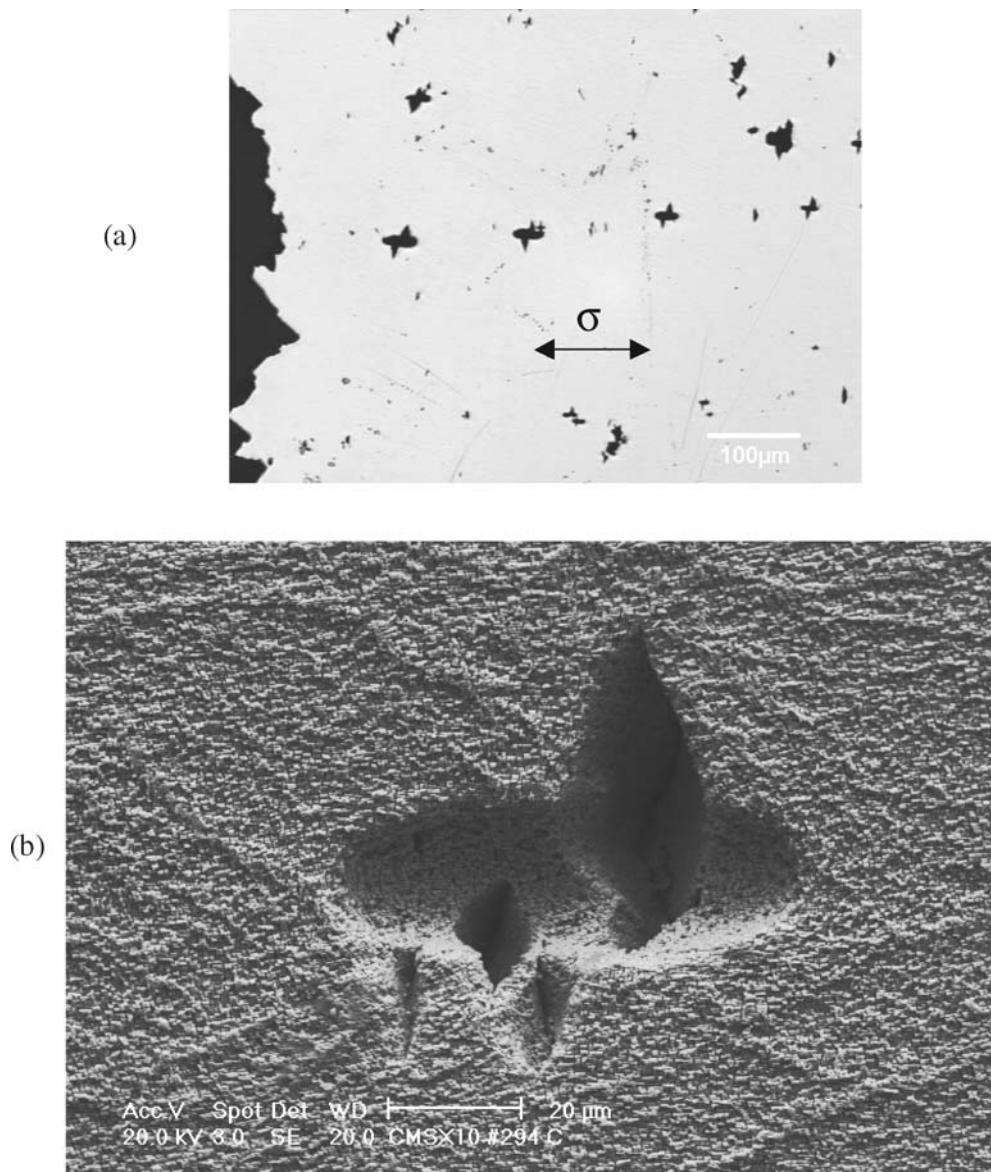


Figure 5 Optical image (a) of a section normal to the fracture surface (at left) for the test at 1173 K and Scanning Electron Micrograph (b) showing cubic  $\gamma'$  precipitates and the wing-cracks associated with a pore elongated during creep in the direction of the stress axis.

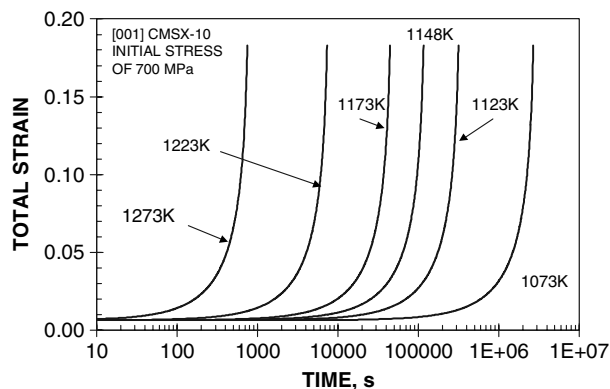


Figure 6 Theoretical results for CMSX-10 for constant-load test,  $\sigma_i = 700$  MPa.

small strains, an elasto-viscous (nonlinear) model, based on Equations 1 and 2 will be applicable for the tertiary stage:

$$\varepsilon = \varepsilon_e + \varepsilon_c = \sigma_A / E + t S_{\text{ref}, T} \left\{ \dot{\varepsilon}_{A(1)} (\sigma_A / \sigma_1)^{n(A)} \right\} \quad (3)$$

For an isothermal constant load test,  $\sigma_A = \sigma_i$  at  $t = 0$ . The creep strain for  $t > 0$ , accumulates with each increment of time,  $\Delta t$  and increases the stress to  $\sigma_A = \sigma_i (1 + \Delta \varepsilon_c)$ , which enhances the creep rate. A numerical program was developed and calculations were made, using  $E = 110$  GPa,  $n(A) = 18.5$  and  $\dot{\varepsilon}_{A(1)} = 1.712 \times 10^{-58}$  (obtained for  $T_{\text{ref}} = 1223$  K in Fig. 3). The results are shown in Fig. 6 for  $\sigma_i = 700$  MPa. This 'reference' curve was then shifted along the time axis [11] to produce the results for other temperatures, using  $S_{\text{ref}, T}$  with  $Q = 430$  kJ mole $^{-1}$  for  $T < T_{\text{ref}}$  and  $Q = 590$  kJ mole $^{-1}$  for  $T > T_{\text{ref}}$  (1273 K). As expected the results in Fig. 6 differ from those in Fig. 1 during the primary creep, giving rise to a requirement for an additional term (to be discussed elsewhere) in Equation 3. However, theoretical results compare extremely well with the experimental results at larger strains or longer times relevant to the 'so-called' tertiary stages of creep. These close agreements tend to give indirect indications that crack-damage enhanced effects must control creep during the final stages of necking and frac-

ture. Space does not allow detailed discussions here, but it should be mentioned here that cracks associated with the pores, as shown in Fig. 5, were seen mainly in the necked-down section in the failed specimens and within a few mm of the fracture surface. Although it is irrelevant to the current analysis, it is interesting to note the close agreement between the experimental results and the corresponding prediction on the increase in the 'incubation time' during early primary creep with the decrease in temperature.

## Acknowledgments

The author is indebted to R. McKellar for performing the creep tests, P. Au for obtaining the test bars from an aeroengine manufacturer, O. Lupandina and W. Chen for their assistance in the metallurgy laboratory.

## References

1. F. R. N. NABARRO and H. L. DE VILLIERS, in "The Physics of Creep" (Taylor & Francis, London, 1995) Chapter 6, p. 187.
2. G. L. ERICKSON, in "Superalloys 1996," edited by R.D., Kissinger, D.J. Deye, D.L. Anton, A.D. Cetel, M.V. Nathal, T.M. Pollock and D.A. Woodford (The Minerals, Metals & Materials Society, 1996), p. 35.
3. F. R. N. NABARRO, *Metall. and Mater. Trans. A* **27A** (1996) 513.
4. N. K. SINHA, *J. Mat. Sci. L.* **20** (2001) 951.
5. H.-A. KUHN and H.-G. SOCKEL, *Mat. Sci. Eng. A* **112** (1989) 117.
6. N. MIURA, Y. KONDO and T. MATSUO, in "Creep and Fracture of Engineering Materials and Structures", edited by J. D. Parker (The Institute of Materials, London, 2001), p. 437.
7. N. MIURA, Y. KONDO and T. MATSUO, *Tetsu-to-Hagane*, **89** (2003) 58.
8. L.-M. PAN, I. SCHEIBLI, M. B. HENDERSON, B. A. SHOLLOCK and M. MCLEAN, *Acta Metall Mater.* **43** (1995) 1375.
9. J. SVOBODA and P. LUKAS, *Acta Mater.* **46** (1998) 3421.
10. R. C. REED, N. MATAN, D. C. COX, M. A. RIST and M. F. RAE, *ibid.* **47** (1999) 3367.
11. N. K. SINHA, *Philos Mag A* **40** (1979) 824.
12. T. M. POLLOCK and A. S. ARGON, *Acta Metall.* **40** (1992) 1.
13. C. KNOBLOCH, V. SAB, D. SIEBORGER and U. GLATZEL, *Mat Sci Eng. A* **234-236** (1997) 237.

Received 23 February  
and accepted 17 May 2005